

# Low-temperature SCR of NO with NH<sub>3</sub> over AC/C supported manganese-based monolithic catalysts

Xiaolong Tang<sup>a,b</sup>, Jiming Hao<sup>a,\*</sup>, Honghong Yi<sup>a,b</sup>, Junhua Li<sup>a</sup>

<sup>a</sup>Department of Environmental Science & Engineering, Tsinghua University, Beijing 100084, China

<sup>b</sup>College of Environmental Science & Engineering, Kunming University of Science & Technology, Kunming 650093, China

Available online 20 July 2007

## Abstract

Metal oxide/active carbon/ceramic (MO<sub>x</sub>/AC/C) monolithic catalysts were prepared by impregnation method for selective catalytic reduction (SCR) of NO<sub>x</sub> with NH<sub>3</sub> at low-temperature, and they also had been characterized by elemental analysis, N<sub>2</sub>-BET, XRD, SEM and NO-TPD. The adsorption capability of the monolithic catalyst was greatly enhanced due to the attached active carbon. An ultrasonic treatment was used to improve the impregnation process, and which can increase their catalytic activities. More than 90% NO<sub>x</sub> conversion could be achieved over the Mn-based monolithic catalysts at low-temperature, and which could be improved further by doping Ce, from 30% to 78% at 100 °C. Mn–Fe–Ce and Mn–V–Ce monolithic catalysts had better tolerance to SO<sub>2</sub> than Mn or Mn–Ce monolithic catalysts.

© 2007 Elsevier B.V. All rights reserved.

**Keywords:** Monolithic catalyst; Active carbon; NO<sub>x</sub>; Ammonia; SCR; Low-temperature

## 1. Introduction

The selective catalytic reduction (SCR) of NO<sub>x</sub> by ammonia is the major technology to reduce nitrogen oxide emissions from stationary sources. The common commercialized industrial catalyst for NO<sub>x</sub>-SCR are V<sub>2</sub>O<sub>5</sub> + WO<sub>3</sub> (MoO<sub>3</sub>)/TiO<sub>2</sub> catalysts, which are operated under 300–400 °C, and substantial work had been done to improve the performance of vanadium type catalysts [1–5]. However, SO<sub>2</sub> and the high concentrations of ash, e.g. K<sub>2</sub>O, CaO and As<sub>2</sub>O<sub>3</sub>, in the flues reduce their performance and durability. Therefore, the trend is to develop low-temperature catalysts capable of working downstream of the dust removal equipment and desulfuration devices for flue gases without the need for reheating. The present work is focused on the study of several transition metals oxides (Fe, Cr, Ni, Cu and Mn), which are among those known to be active in the low-temperature deNO<sub>x</sub> SCR reaction (Fe [6–8], Cr [9,10], Ni [11], Cu [6,12–14] and Mn [7,15–23,29–31]).

Carbon had been studied as the catalyst support for the low-temperature NO<sub>x</sub>-SCR by many researchers due to its high specific area and its chemical stability. These investigations

included many types of carbon materials, granular active carbon (GAC) [7], activated carbon fibers (Nomex-based ACFs) [22,23], A-572 active carbon [24], chars and activated chars [25], carbonized resin [6,17], fluorinated carbon fibers [26] and commercial coal-derived semi-coke [27,28].

In this work, an effective method was developed to prepare active carbon support (AC/C) [29]. Monolithic catalysts were prepared by impregnation of AC/C with certain aqueous solutions of nitrate (Mn, Fe and Cu), and ultrasonic treatment was used to improve this process. Mn-based catalysts showed good activity for NO<sub>x</sub>-SCR with NH<sub>3</sub> at low temperature, and they were characterized by elemental analysis, N<sub>2</sub>-BET, XRD, SEM and NO-TPD.

## 2. Experimental

### 2.1. Catalyst preparation

The ceramic honeycomb support was cut into small column samples, which were 15 mm in length and 12 mm in diameter. After pretreatment with nitric acid solution (40 vol.%) and washing with the de-ionized water, these supports were immersed into the mixed resin solution (PF resins, polyethylene glycol and propanone). Then, the support was flushed with compressed air to remove the excess solution in the channels,

\* Corresponding author. Tel.: +86 10 6278 2195; fax: +86 10 6277 3650.

E-mail address: [hjm-den@tsinghua.edu.cn](mailto:hjm-den@tsinghua.edu.cn) (J. Hao).

and cured in air (100 °C, 30 min). The following steps of AC/C support manufacturing process were described in Ref. [17]. In our work, the carbon content of the final AC/C support was 12–14 wt.%. There were four steps in the active components loading procedure: (i) equilibrium adsorption impregnation of metal nitrate solution; (ii) use of ultrasonic to enhance the loading and the dispersion procedure; (iii) washing with the de-ionized water and drying at 100 °C for 1 h; and (iv) calcining in N<sub>2</sub> at 400 °C for 1 h. The former three steps were adopted in order to maximize the dispersion and loading of metal oxides, and the active sites were formed in the final step.

It is well known that the balance between dispersion and loading of metal oxides is a key factor, which impacts the catalyst activity directly. Increasing the metal oxide loading will result in the aggregation of metal oxides to decrease the dispersion; however, low loading could ensure good dispersion, but the quantity of the active sites over the support will also be too little. Preliminary testing about the loading of metal oxides had been carried out, and the results showed that loading at 8–10 wt.% is best. All of the catalysts in this work were prepared by same methodology; the loading of metal oxides was controlled at 8 wt.%.

## 2.2. Catalyst characterization

BET-surface areas were measured by N<sub>2</sub> adsorption using a NOVA4000 automated gas sorption system. X-ray diffraction (XRD) measurements were carried out on D8 Advance X-ray diffractometer with Cu K $\alpha$  radiation. Before the XRD test, the catalyst should be crushed and ground. A scanning electron microscope (HITACHI, S-450) was used to collect the surface information of the monolithic catalyst.

Temperature programmed desorption (TPD) experiments of NO were performed by using a monolithic catalyst. The desorbed samples were monitored continuously by a Quintox Flue Gas Analyzer (KM9106, Kane-May). Prior to the TPD-NO experiment, the catalyst sample was pre-treated in a flow of 3% O<sub>2</sub>/N<sub>2</sub> at 250 °C for 1 h and then cooled down to room temperature. Chemisorption of NO was performed by passing a flow of 500 ppm NO/N<sub>2</sub> through the catalyst at room temperature for 1 h. Afterward, the sample was purged in N<sub>2</sub> until no NO was detected, and the TPD measurements were carried out up to 450 °C with a heating rate of 10 °C min<sup>-1</sup> in flowing N<sub>2</sub>. The gas flow rate was fixed at 300 cm<sup>3</sup> min<sup>-1</sup>. The amount of NO desorption from catalyst was quantified by calibrating the peak area against that of a standardized NO pulse.

## 2.3. Catalytic activity measurement

Catalytic activity tests were performed in a quartz tube reactor of 12 mm internal diameter. NO<sub>x</sub>, O<sub>2</sub> and SO<sub>2</sub> concentration in the inlet and outlet gases were simultaneously measured by Quintox Flue Gas Analyzer (KM9106, Kane-May). At steady state, a gas N<sub>2</sub> mixture containing 500 ppm NO, 550 ppm NH<sub>3</sub>, 3% O<sub>2</sub>, 100 ppm SO<sub>2</sub> (when used) was introduced into the reactor. In all tests, the total flow rate was

controlled at 300 cm<sup>3</sup> min<sup>-1</sup>, which corresponded to a gas hourly space velocity (GHSV) of 10,610 h<sup>-1</sup> (based on the monolith volume). NO<sub>x</sub> conversion was obtained by following equation:

$$\text{NO}_x \text{ conversion (\%)} = \left[ 1 - \frac{(\text{NO} + \text{NO}_2)_{\text{outlet}}}{(\text{NO} + \text{NO}_2)_{\text{inlet}}} \right] \times 100$$

## 2.4. NO oxidation to NO<sub>2</sub>

Some previous experiments indicated that the oxidation of NO to NO<sub>2</sub> is important to low-temperature SCR [7,18,20]. Increasing the O<sub>2</sub> content of the airflow could improve NO oxidation, which also could be achieved by doping with another metal element to enhance the oxidizability of catalyst [18]. An oxidation capability investigation for each catalyst would be helpful to further the catalytic mechanism study.

The experiment of NO oxidation to NO<sub>2</sub> was performed in a fix-bed quartz reactor. Samples of each metal oxide (0.2 g) were used and the conversion at each temperature was obtained after 1 h at steady state.

## 3. Results and discussion

### 3.1. Characterizations of catalysts

The BET-surface area, pore volume, and pore size of monolithic catalysts were summarized in Table 1. The surface areas were 5.08, 101.3 and 88.71 m<sup>2</sup>/g for bared ceramic, AC/C and MnO<sub>x</sub>/AC/C. The results showed that the surface area of ceramic support is enhanced greatly by attached AC. Due to calcination, the surface area, pore volume and average pore diameter of all monolithic catalyst samples decreased after the active component loading process.

The adsorption of NO was enhanced greatly because of the attached active carbon, as shown in Fig. 1. The attached AC will increase NH<sub>3</sub> adsorption and activation, and much work had been done to indicate that it is a key step in the low-temperature SCR reaction [30–32]. Due to the limited surface area, the TPD profile of bare ceramic only shows a small peak at 80 °C, and soon disappears. In case of MnO<sub>x</sub>/AC/C, one large desorption peak appears at a relative high temperature, 200 °C. The AC/C shows a different TPD profile in which two distinct desorption peaks of NO are observed. The first large peak is centered at about 180 °C and the second one is centered at 400 °C. The amounts of NO desorption calculated based on the results of

Table 1  
Characterization of the catalysts

Samples	BET-surface area (m <sup>2</sup> /g)	Pore volume (cm <sup>3</sup> /g)	Average pore diameter (nm)
Bared ceramic	5.08	0.051	4.01
AC/C	101.3	0.078	3.05
MnO <sub>x</sub> /AC/C	88.71	0.057	2.56
MnO <sub>x</sub> -CeO <sub>2</sub> /AC/C	79.61	0.053	2.55
CuO/AC/C	82.77	0.052	2.56

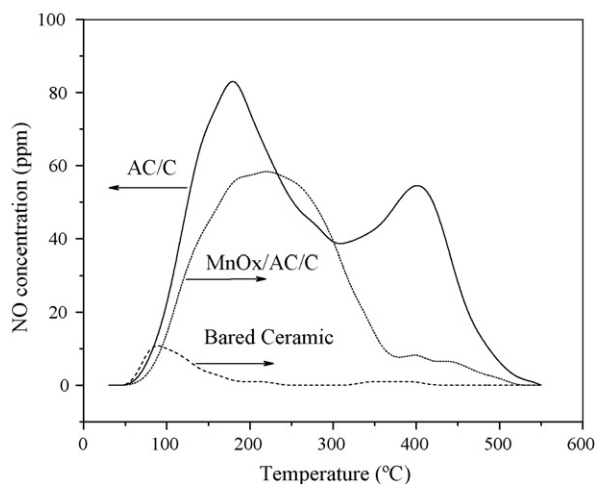


Fig. 1. TPD profiles of NO on bare ceramic (dash line), AC/C (solid line) and  $\text{MnO}_x/\text{AC}/\text{C}$  (dot line). Conditions: TPD measurements were carried out up to 550 °C with a heating rate of 10 °C  $\text{min}^{-1}$  in flowing  $\text{N}_2$ . The gas flow rate was fixed at 300  $\text{cm}^3 \text{min}^{-1}$ .

Fig. 1 are 1.23, 16.82 and 27.42  $\mu\text{mol g}^{-1}$  for bare ceramic,  $\text{MnO}_x/\text{AC}/\text{C}$  and AC/C. The attached AC over the monolithic catalyst results in an increase in the amount of NO chemisorption. This is especially obvious over fresh AC/C supports.

Four samples with different  $\text{MnO}_x$  loading, 2.5, 5, 8 and 15 wt.%, were analyzed by X-ray diffraction. In Fig. 2, the XRD profiles of the former three samples have no characteristic peaks of manganese oxides. Until the loading increases to 15 wt.%, the manganese oxides could be detected, mainly as  $\text{Mn}_2\text{O}_3$ . Therefore, in this work all monolithic catalysts were prepared at an appropriate metal oxides loading value, 8 wt.%, suggesting that the active sites will be well dispersed on the catalysts.

Further surface information of the catalysts were shown in the followed SEM photos (Fig. 3). The surface of bare ceramic (Fig. 3A) was coarse and there were many macropores on its surface, which would encourage the metal oxides to be dispersed unevenly. The surface of AC/C (Fig. 3B) was improved by the

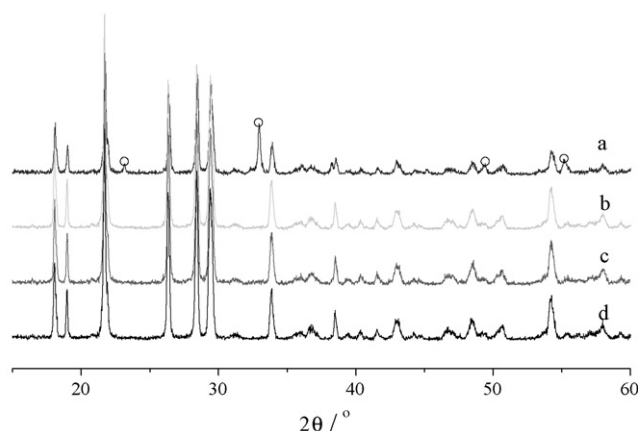


Fig. 2. XRD patterns of  $\text{MnO}_x/\text{AC}/\text{C}$  with different manganese oxides loading. The manganese oxides loading of monolithic catalysts are 15%, 8%, 5% and 2.5% (wt.%) to sample a, b, c and d. All samples had been crushed and ground before XRD test.

attached AC, which became smoother than it had been, and the rate of mesopores and micropores increased. The partially enlarged photographs of bare ceramic and AC/C (Fig. 3a and b) show more clearly that the amounts of macropores decreased on the surface of AC/C. In another catalyst stability test, we found that the attached AC would be lost by oxidation, at relative high temperature (>250 °C). As Fig. 3C shows, more macropores appeared and some slight AC pieces fell out; each of these phenomena would cause the deactivation of monolithic catalysts. Furthermore, many small particle materials were observed on the monolithic catalyst surface after  $\text{SO}_2$  deactivation testing (as Fig. 3c showed), which might be sulfate, i.e.  $(\text{NH}_4)_2\text{SO}_4$ . This indicates that one aspect of the  $\text{SO}_2$  deactivation of the monolithic catalyst was due to the active sites on the catalyst surface were covered by the sulfate particles, and the SCR reaction could not carried out effectively.

### 3.2. Effect of ultrasonic treatment

In the preparation of the catalysts, the ultrasonic treatment was used to improve the impregnation procedure, and which has significant effect on the catalytic activity of monolithic catalyst at low-temperature. In case of  $\text{MnO}_x/\text{AC}/\text{C}$  impregnation without ultrasonic treatment, the best loading of manganese oxides is only 2 wt.% (Fig. 4), and after this the activity would decrease as loading increased, especially after 200 °C.

The best loading of manganese oxides was 8 wt.% with aid of ultrasonic treatment for the impregnation. The low-temperature catalytic activity improved greatly; the  $\text{NO}_x$  conversion increased from 52% to 77% at 150 °C (Fig. 5), but showed almost no variation at high temperature (>200 °C). This is mainly due to the ultrasonic treatment that enhanced the metal component dispersion on the catalyst surface during the impregnation procedure, which results in the increase of active sites on the catalyst surface.

At low-temperature, the SCR reaction rate is slow, so the increasing of the amount of the active sites over the catalyst surface is very important to improve the catalytic activity; but with the reaction temperature rising, this positive impact will be weakened due to the reaction rate speedup.

### 3.3. Catalytic activity

Some catalysts supported on active carbon showed good low-temperature activity, e.g.  $\text{PFCu}$ ,  $\text{PFFe}$  [6],  $\text{V}_2\text{O}_5/\text{AC}$  [27] and  $\text{MnO}_x/\text{AC}/\text{C}$  [29]. Besides, the  $\text{MnO}_x\text{--CeO}_2$  catalyst was reported for its superior catalytic activity at 100–150 °C, and doped Fe or Pr could improve its resistance to  $\text{SO}_2$  [18]. So, in this work we prepared series of metal oxide monolithic catalysts, besides above-mentioned metal elements, also investigated noble metal, Pd and Pt. The activity data are summarized in Fig. 6.

As shown in Fig. 6, in single metal oxide catalysts,  $\text{Mn}/\text{AC}/\text{C}$  has better low-temperature activity than others (Cu, Fe and V). More than 90%  $\text{NO}_x$  conversion could be achieved at 180 °C over the  $\text{Mn}/\text{AC}/\text{C}$  catalyst, but only 51%, 35% and

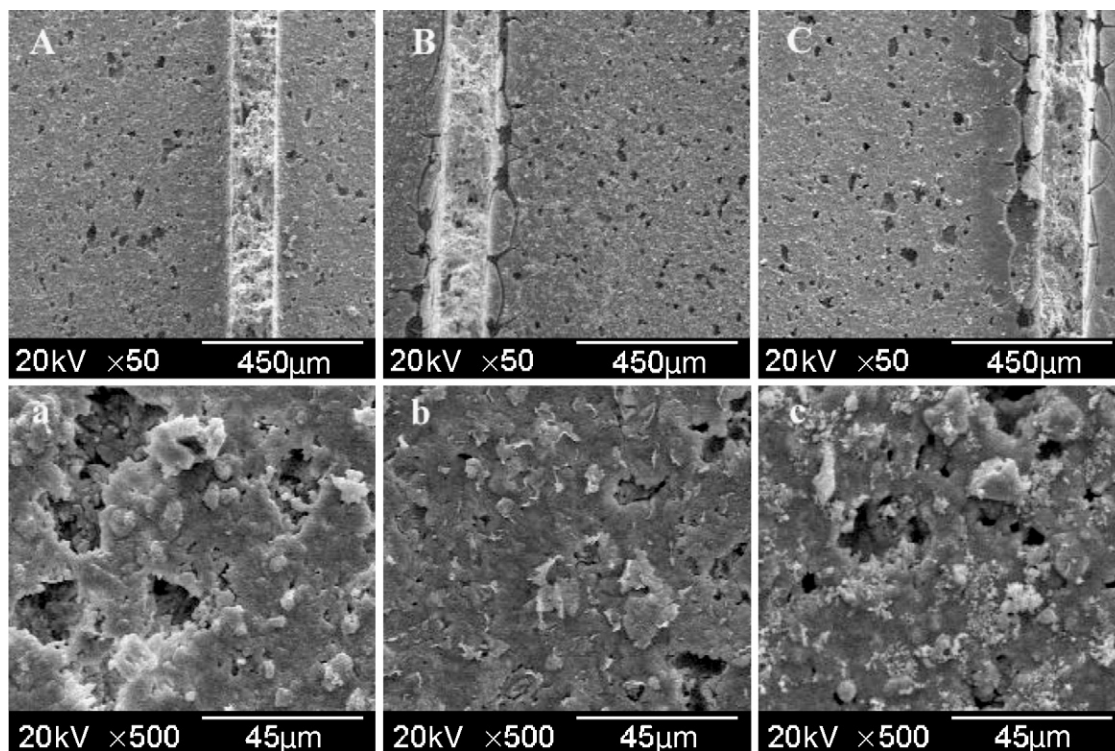


Fig. 3. SEM photos of monolithic catalysts. (A) Bare ceramic support; (B) fresh  $\text{MnO}_x/\text{AC}/\text{C}$  catalyst; (C)  $\text{MnO}_x/\text{AC}/\text{C}$  after stability activity test; (a) part of A; (b) part of B; (c)  $\text{MnO}_x/\text{AC}/\text{C}$  after  $\text{SO}_2$  test.

38% over the  $\text{Cu}/\text{AC}/\text{C}$ ,  $\text{Fe}/\text{AC}/\text{C}$  and  $\text{V}/\text{AC}/\text{C}$  catalysts, respectively.

In order to decrease the loss of the active carbon, we tried to improve the low-temperature activity of the catalyst. The low-temperature activity of the Mn-based monolithic catalyst is enhanced by doped cerium, as showed in Fig. 6. Near 80%  $\text{NO}_x$  conversion could be achieved at 100 °C and more than 90% conversion occurred in a broad temperature range. Besides, noble metal is also considered to improve the SCR catalytic activity of  $\text{MnO}_x\text{-CeO}_2/\text{AC}/\text{C}$  at even lower temperature. The impact of Pd and Pt are reverse. Pd component doping can

improve the low-temperature catalytic activity (100–150 °C), but the promotion is slight. Contrary, when Pt doped, the catalytic activity is abated obviously, which may due to the  $\text{NH}_3$  oxidation was promoted extremely by Pt component.

More than 90%  $\text{NO}_x$  conversion can be achieved over  $\text{MnO}_x$ -based monolithic catalysts (except  $\text{Pt-MnO}_x\text{-CeO}_2/\text{AC}/\text{C}$ ), and their low-temperature (<200 °C) SCR activity decreased in the following sequence:  $\text{Pd-MnO}_x\text{-CeO}_2/\text{AC}/\text{C} > \text{MnO}_x\text{-CeO}_2/\text{AC}/\text{C} > \text{MnO}_x/\text{AC}/\text{C}$ .

Though high  $\text{NO}_x$  conversion also could be achieved over  $\text{CuO}$  and  $\text{V}_2\text{O}_5$  monolithic catalysts, the operating temperature

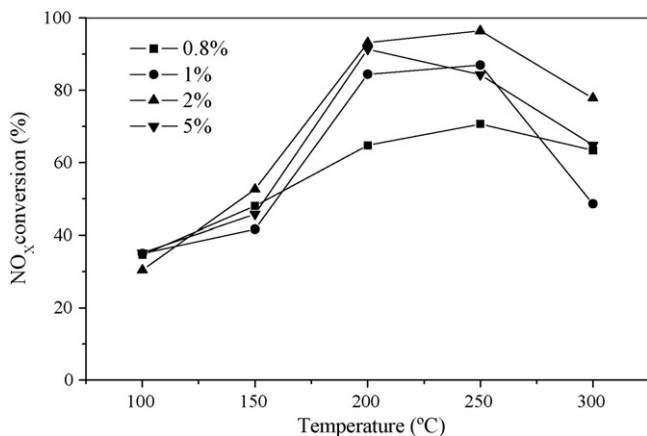


Fig. 4. Activity test of  $\text{MnO}_x/\text{AC}/\text{C}$  with different  $\text{MnO}_x$  loading (without ultrasonic treatment). Conditions: 500 ppm  $\text{NO}$ , 550 ppm  $\text{NH}_3$ , 3%  $\text{O}_2$ ,  $\text{N}_2$  to balance, GHSV = 10,600  $\text{h}^{-1}$ .

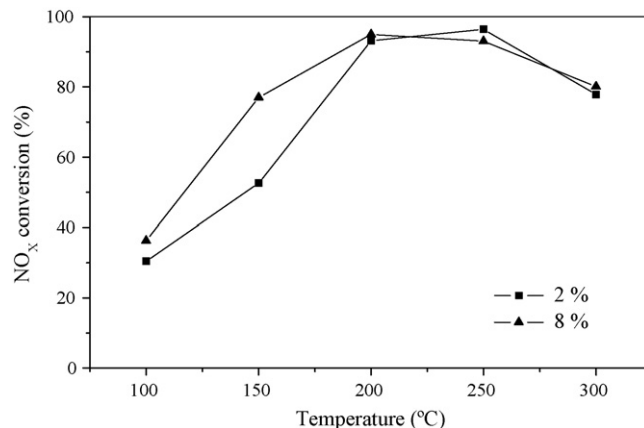


Fig. 5. Catalytic activity comparison of two monolithic catalysts. One was prepared by normal impregnation method, and the best loading of  $\text{MnO}_x$  is 2 wt.%. Another was prepared by improved impregnation method (with ultrasonic treatment); the best loading of  $\text{MnO}_x$  is 8 wt.%. Conditions: 500 ppm  $\text{NO}$ , 550 ppm  $\text{NH}_3$ , 3%  $\text{O}_2$ ,  $\text{N}_2$  to balance, GHSV = 10,600  $\text{h}^{-1}$ .



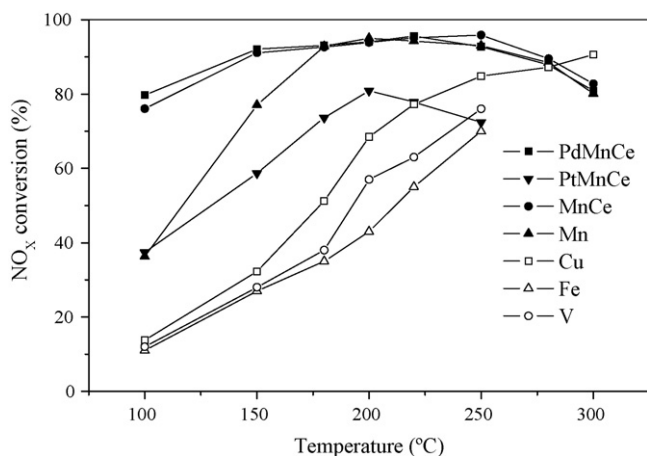


Fig. 6. Catalytic activity comparison of different metal oxides supported on AC/C cellular monolithic catalysts. Conditions: 500 ppm NO, 550 ppm NH<sub>3</sub>, 3% O<sub>2</sub>, N<sub>2</sub> to balance, GHSV = 10,600 h<sup>-1</sup>.

were relative high (>300 °C). High temperature is adverse to the catalyst durability; because the attached AC will be oxidized into CO<sub>2</sub>/CO, a reaction accelerated at high temperature.

### 3.4. Effect of O<sub>2</sub>

O<sub>2</sub> is important in the SCR reaction, especially at low temperature. The prior research about the SCR mechanism over MnO<sub>x</sub>-CeO<sub>2</sub> [20] indicates that the NO oxidation to NO<sub>2</sub> and NH<sub>3</sub> activation to NH<sub>2</sub>/OH are the key steps in the SCR reaction. Increasing O<sub>2</sub> content or enhancing the oxidizing capability of the catalyst both can improve these two steps. The following experiments were carried out to investigate the effect of O<sub>2</sub> at different temperature over MnO<sub>x</sub>/AC/C catalyst.

As Fig. 7 shows, the promoter action of O<sub>2</sub> was obvious at low temperature, 100–150 °C. The NO<sub>x</sub> conversion was only 17.1% at 100 °C when the O<sub>2</sub> content was 1%, however, it could achieve 46.3% with 7% O<sub>2</sub>. But the improvement of O<sub>2</sub> will be slight as the reaction temperature rises. At 200 °C, the profiles show almost no change with different O<sub>2</sub> content.

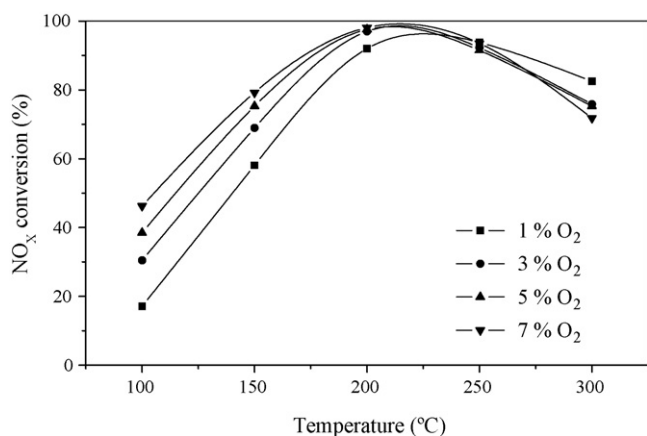


Fig. 7. Effect of O<sub>2</sub> concentration on catalytic performance on MnO<sub>x</sub>/AC/C. Conditions: 500 ppm NO, 550 ppm NH<sub>3</sub>, 1–7% O<sub>2</sub>, N<sub>2</sub> to balance, GHSV = 10,600 h<sup>-1</sup>.

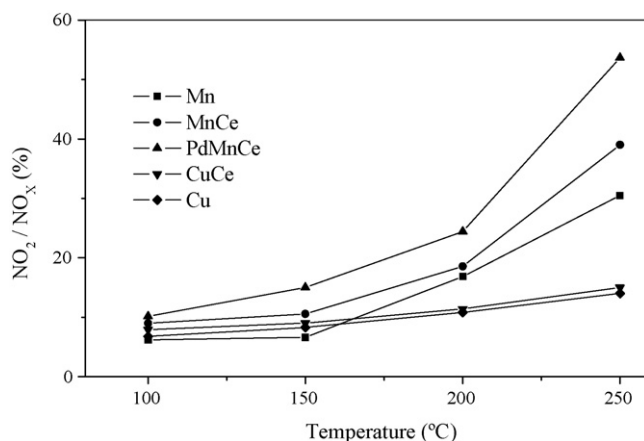


Fig. 8. Oxidation activity of NO to NO<sub>2</sub> by O<sub>2</sub> on different metal oxides catalysts. Conditions: 0.2 g samples, 500 ppm NO, 3% O<sub>2</sub>, N<sub>2</sub> to balance, GHSV = 70,700 h<sup>-1</sup>.

The importance of O<sub>2</sub> was also verified by a similar work of Qi and Yang [18]. Transient behavior of the catalyst was tested by turning the O<sub>2</sub> off and on in the gas flow. The test showed that the NO conversion declined quickly after O<sub>2</sub> was turned off, but it could be restored by switching the O<sub>2</sub> back on.

### 3.5. NO oxidation to NO<sub>2</sub>

The oxidation activities of NO to NO<sub>2</sub> by O<sub>2</sub> on certain metal oxides (powder) were measured (Fig. 8), and all samples were prepared by the citric acid method [18]. On MnO<sub>x</sub>-based catalysts, though, the oxidation activities of NO to NO<sub>2</sub> were limited at low temperature, but quickly increased with rising temperature. As Fig. 8 shows, after Ce and Pd were doped, the oxidization of NO to NO<sub>2</sub> was greater than before. However, the oxidizing capability of CuO and CuO-CeO<sub>2</sub> are very low, and almost no variation occurred with changing the temperature.

### 3.6. SO<sub>2</sub> deactivation

In order to evaluate the effect of SO<sub>2</sub> on catalytic activity, catalytic tests in which SO<sub>2</sub> 100 ppm was added to the feed gas were performed at 200 °C.

The results of experiments are plotted in Fig. 9, in which the bars indicate the ratio of NO<sub>x</sub> conversions ( $X/X_0$ , SO<sub>2</sub> were added) to the initial conversion ( $X_0$ , without SO<sub>2</sub>). In our tests, the catalytic activity of all monolithic catalysts was decreased, and only V<sub>2</sub>O<sub>5</sub>/AC/C performed better. Though MnO<sub>x</sub>/AC/C and MnO<sub>x</sub>-CeO<sub>2</sub>/AC/C had good low-temperature activity, both were easily deactivated by SO<sub>2</sub>. Doping the MnO<sub>x</sub>-based monolithic catalysts with Fe or V improved the resistance to SO<sub>2</sub>, but the value of  $X/X_0$  was still not ideal, only 51% when doped with Fe and 56% when doped using V. Furthermore, their activity could not be restored when SO<sub>2</sub> was turned off.

When these observations were combined with the SEM photo, Fig. 3c, the SO<sub>2</sub> deactivation of catalysts might have two causes. On one hand, the metal oxides on the supports, acting as

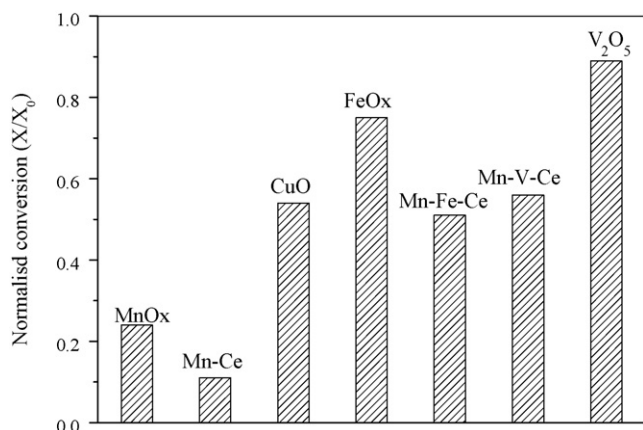


Fig. 9. Effect of SO<sub>2</sub> on activities on different monolithic catalysts. Conditions: 500 ppm NO, 550 ppm NH<sub>3</sub>, 100 ppm SO<sub>2</sub>, 3% O<sub>2</sub>, N<sub>2</sub> to balance, 200 °C, GHSV = 10,600 h<sup>-1</sup>.

active sites of the monolithic catalyst, were sulfated by SO<sub>2</sub> and lost activity. Alternatively, the reductant (NH<sub>3</sub>) reacted with SO<sub>2</sub> and produced (NH<sub>4</sub>)<sub>2</sub>SO<sub>4</sub>. Along with the reaction, more and more (NH<sub>4</sub>)<sub>2</sub>SO<sub>4</sub> particles formed and deposited on the catalyst's surface, covering many active sites, which resulted in a blocking of the SCR reaction. The first effect of SO<sub>2</sub> was irreversible, but subsequent impacts could be eliminated by washing to remove the deposited (NH<sub>4</sub>)<sub>2</sub>SO<sub>4</sub> or heating at relative high temperature to decompose it.

In other investigations [16,17,33,34], the results indicated that the deactivation of SO<sub>2</sub> will be weak with increasing temperature, and interestingly, adding SO<sub>2</sub> could improve the SCR reaction after 300 °C, but not at low temperature (<200 °C).

#### 4. Conclusion

The present work has shown that the MnO<sub>x</sub>-based monolithic catalysts are more active than other metal oxide catalysts for low-temperature SCR reactions of NO with NH<sub>3</sub> in the presence of excess oxygen. More than 90% NO<sub>x</sub> conversion was obtained over the range of 150–250 °C under the condition of GHSV = 10,600 h<sup>-1</sup>. During the catalyst preparation, ultrasonic treatment can promote the dispersion of metal oxides on the surface of the AC, and improve the low-temperature catalytic activity, especially at 150 °C (Fig. 5). The investigation of O<sub>2</sub> effect and the oxidation of NO to NO<sub>2</sub> on monolithic catalysts both indicate that NO oxidation is one of the essential factors of low-temperature SCR reaction. Doping with Ce and Pd can improve the MnO<sub>x</sub>-based monolithic catalysts, and result in the SCR reaction being performed more effectively. The tolerance to SO<sub>2</sub> of MnO<sub>x</sub>-based catalysts could be enhanced by doping with Fe and V, and more than 50% of the catalytic activity could remain under conditions of 100 ppm SO<sub>2</sub> in the flue gas. The deactivation of SO<sub>2</sub> might be caused by two reasons, metal oxides sulfuration which is irreversible or (NH<sub>4</sub>)<sub>2</sub>SO<sub>4</sub> deposition.

#### Acknowledgements

This work was financially supported by the Key Project of the Natural Science Foundation of China (20437010), the National 863 Project of China (2004AA649150), the Natural Science Foundation of Yunnan Province and Foundation of Kunming University of Science & Technology (14118052).

#### References

- [1] B. Stefan, H. Thomas, Appl. Catal. B 28 (2000) 101–111.
- [2] S. Djerad, L. Tifouti, M. Crocoll, W. Weisweiler, J. Mol. Catal. A: Chem. 208 (2004) 257–265.
- [3] S.T. Choo, S.D. Yim, I.S. Nam, S.W. Ham, J.B. Lee, Appl. Catal. B 44 (2003) 237–252.
- [4] V.I. Pârvulescu, S. Boghosian, V. Pârvulescu, S.M. Jung, P. Grange, J. Catal. 217 (2003) 172–185.
- [5] N. Macleod, R.M. Lambert, Catal. Lett. 90 (2003) 111–115.
- [6] H. Teng, L.Y. HSU, Y.C. Lai, Environ. Sci. Technol. 35 (2001) 2369–2374.
- [7] M. Yosikawa, A. Yastutake, I. Mochida, Appl. Catal. A 173 (1998) 239–245.
- [8] G. Ramis, M.A. Larrubia, J. Mol. Catal. A: Chem. 215 (2004) 161–167.
- [9] M.J. Illan-Gomez, A. Linares-Solano, C. Salinas-Martinez de Lecea, Energy Fuel 9 (1995) 976–983.
- [10] B.L. Duffy, H.E. Curry-Hyde, N.W. Cant, P.F. Nelson, Appl. Catal. B 5 (1994) 133–147.
- [11] J. Blanco, P. Ávila, S. Suárez, J.A. Martín, C. Knapp, Appl. Catal. B 28 (2000) 235–244.
- [12] J. Blanco, P. Ávila, S. Suárez, M. Yates, J.A. Martín, L. Marzo, C. Knapp, Chem. Eng. J. 97 (2004) 1–9.
- [13] G. Centi, S. Perathoner, D. Biglino, E. Giamell, J. Catal. 152 (1995) 75–92.
- [14] G. Ramis, L. Yi, G. Busca, M. Turco, E. Kotor, R.J. Willey, J. Catal. 157 (1995) 523–535.
- [15] K. Krishna, G.B.F. Seijger, C.M. van den Bleek, H.P.A. Calis, Chem. Commun. 18 (2002) 2030–2031.
- [16] T.S. Park, S.K. Jeong, S.H. Hong, S.C. Hong, Ind. Eng. Chem. Res. 40 (2001) 4491–4495.
- [17] T. Valdés-Solís, G. Marbán, A.B. Fuertes, Appl. Catal. B 46 (2003) 261–271.
- [18] G. Qi, R.T. Yang, J. Catal. 217 (2003) 434–441.
- [19] W.S. Kijlstra, J.C.M.L. Daamen, J.M. van de Graaf, B. Van de Linden, E.K. Poels, A. Bliet, Appl. Catal. B 7 (1996) 337–357.
- [20] G. Qi, R.T. Yang, R. Chang, Appl. Catal. B 51 (2004) 93–106.
- [21] M. Kantcheva, J. Catal. 204 (2001) 479–494.
- [22] G. Marbán, A.B. Fuertes, Appl. Catal. B 34 (2001) 43–53.
- [23] G. Marbán, A.B. Fuertes, Appl. Catal. B 34 (2001) 55–71.
- [24] K. Jurczyk, R.S. Drago, Appl. Catal. A 173 (1998) 145–151.
- [25] M.J. Lázaro, M.E. Gálvez, I. Suelves, R. Moliner, S.V. Vassilev, C. Braekman-Danheux, Fuel 83 (2004) 875–884.
- [26] W. An, Q.L. Zhang, K.T. Chuang, A.R. Sanger, Ind. Eng. Chem. Res. 41 (2002) 27–31.
- [27] Z.G. Huang, Z.P. Zhu, Z.Y. Liu, Appl. Catal. B 39 (2002) 361–368.
- [28] Z.P. Zhu, Z.Y. Liu, S.J. Liu, H.X. Niu, Appl. Catal. B 23 (1999) L229–L233.
- [29] T. Valdés-Solís, G. Marbán, A.B. Fuertes, Catal. Today 69 (2001) 259–264.
- [30] M. Richter, A. Trunschke, U. Bentrup, K.W. Brzezinka, E. Schreier, M. Schneider, M.M. Pohl, R. Fricke, J. Catal. 206 (2002) 98–113.
- [31] W.S. Kijlstra, D.S. Brands, H.I. Smit, E.K. Poels, A. Bliet, J. Catal. 171 (1997) 219–230.
- [32] G. Delahay, S. Kieger, N. Tanchoux, P. Trems, B. Coq, Appl. Catal. B 52 (2004) 251–257.
- [33] S. Okazaki, M. Kumasaka, J. Yoshida, K. Kosaka, Ind. Eng. Chem. Prod. Res. Dev. 20 (1981) 301–305.
- [34] W.B. Li, R.T. Yang, K. Krist, J.R. Regalbuto, Energy Fuel 11 (1997) 428–432.